IIETA International Information and Engineering Technology Association
Advancing the World of Information and Engineering

Traitement du Signal
Vol. 41, No. 5, October, 2024, pp. 2701-2709
Journal homepage: http://iieta.org/journals/ts

Alzheimer's Disease MRI Brain Segmentation Using Pythagorean Fuzzy Sets

Vunnam Asha Latha[1*], Anupama Namburu[1,2]

[1] School of Computer Science Engineering, VIT-AP University, Guntur 522237, India
[2] School of Engineering, Jawaharlal Nehru University, New Delhi 110067, India

Corresponding Author Email: ashalatha.20phd7020@vitap.ac.in

https://doi.org/10.18280/ts.410543

Received: 29 September 2023
Revised: 16 March 2024
Accepted: 15 June 2024
Available online: 31 October 2024

Keywords:
Alzheimer's disease (*AD*), *cerebrospinal fluid* (*CSF*), *Pythagorean fuzzy sets* (*PFS*), *grey matter* (*GM*), *white matter* (*WM*), *medical image segmentation*

ABSTRACT

Alzheimer's disease (AD) is a degenerative and ultimately fatal brain disorder for which there is no cure. This neurological condition, with a complex etiology, causes dementia and cognitive decline, making its identification challenging due to the variation in brain MRIs, including differences in size, shape, and CSF flow. While there is no treatment for AD, its progression can be slowed with early diagnosis. Many researchers have employed image processing-based techniques to differentiate between normal and AD-affected patients based on brain images. However, the brain's regions often look super similar, making it tricky to pinpoint specific areas, plus there's always some uncertainty when it comes to extracting the exact regions. There have been various proposals in the literature for fuzzy c-means and intuitionistic fuzzy c-means (IFCM) approaches to deal with this ambiguity and uncertainty. In contrast, Pythagorean fuzzy sets (PFS) provide a more precise means of verifying membership, making them an effective tool for managing uncertainty. The author analyzed PFS and applied fuzzy c-means to propose Pythagorean fuzzy c-means (PFCM). Additionally, histogram-based initial centroids were used to avoid the local minima problem, which is common in many clustering algorithms. The proposed clustering algorithm demonstrated improved performance, completing execution in less than 1.5 seconds, owing to the incorporation of initial centroids and PFS-based clustering. The proposed method achieved high accuracy rates: 98.64% for white matter (WM), 97.4% for gray matter (GM), and 98.14% for cerebrospinal fluid (CSF) in detecting brain tissues.

1. INTRODUCTION

AD is a classic degenerative age-related disorder. Memory loss, mood swings, cognitive decline, and difficulties in speaking, writing, and walking are all symptoms observed in clinical practice. It is a major disease that threatens the health of elderly people [1]. More than 50 million individuals worldwide are currently affected and is expected to rise to 150 million by 2050. Currently, there is no therapy for AD in humans because the pathogenic mechanism has not been fully explained. One major reason is that dementia is difficult to diagnose because, by the time noticeable memory loss and neurological impairment have set in, the disease is in an irreversibly advanced stage [2]. First, there is an asymptomatic period, followed by moderate cognitive impairment (MCI), which eventually progresses into full-blown Alzheimer's disease. Mild cognitive impairment is frequently misdiagnosed as a natural part of aging and the treatment is delayed. Delaying the onset of AD, altering the course of the disease, and avoiding early intervention measures depend on a correct diagnosis. Hence, the development of novel and effective treatments for Alzheimer's disease depends on its early identification.

Neuronal damage in dementia is permanent, and the resulting structural alterations in the brain can be studied using multifractal frameworks [3]. Many in-depth studies on this condition have been conducted in recent years using computer-aided diagnostics. Early diagnosis of AD has shown better detection results by combining the dimensionality reduction of features method with an efficient classifier, and most studies have followed this trend. There is some indication that Ada-SVM outperforms AdaBoost and Free Surfer in extracting the hippocampus border from the brain image, as demonstrated by Morra et al. [4]. Farhana's research focused on early-stage AD and how to back up the disease's multistage categorization. MRI images were preprocessed (using watershed segmentation and median filtering), and automatic feature extraction was performed using models of convolutional neural networks (CNNs) that were pre-trained with benchmarks, including Alex Net, VGG16, VGG19, ResNet18, and ResNet50. The healthcare business generates massive volumes of data, and algorithm-based systems are essential for making sense of it and improving prediction and diagnosis [5]. In AD, most brain MRI scans are segmented using deep network models trained on CNN data. However, identifying Alzheimer's from the brain structure is complex because of the tissue's penetration; hence, the segmentation of tissues from the brain and then applying classification on the extracted tissues to enhance the prediction of Alzheimer's.

Fuzzy sets address the problem of vagueness by providing a degree of belongingness and non-belongingness [6, 7]. Many algorithms, namely bias-corrected FCM, enhanced FCM,

Kerneled FCM, spatially contained FCM, possibilistic FCM, FCM with spatial information, fuzzy local information C-means, robust kernelized FCM, automatic FCM, meta-heuristic based FCM, and fast generalized FCM based on the fuzzy sets for brain image segmentation were available in the literature [8]. These algorithms effectively handle the vagueness of the images. Rough sets have been suggested to deal with the uncertainty in tissue borders [9, 10]. The algorithms yielded enhanced outcomes in comparison to fuzzy sets and demonstrated the ability to tackle the noise found in the regions [11].

A powerful tool, namely, soft sets (SS) with a mathematical foundation, was proposed by Molodstov to address uncertainty. The parameterization tool in soft sets aids decision-making and has been applied in the medical field. Maji et al. [12] defined and investigated many foundational concepts of soft set theory. They also generalized fuzzy soft sets (FSSs) from crisp soft sets. Soft sets have been applied to brain image segmentation using soft fuzzy c-means [13]. However, the proposed model was ineffective at reducing noise in the images. Intuitionistic fuzzy sets (IFS) with three-degree memberships were proposed as a solution to noise and uncertainty. These degrees include deterministic, non-deterministic, and hesitancy, which were used for clustering [14]. To incorporate local spatial information in an intuitive fuzzy manner, Atanassov [15] suggested that an enhanced intuitionistic fuzzy set is a novel approach. Dubey et al. [16] proposed a rough set based on IFS for segmenting brain MRI images. Verma et al. [17] suggested an enhanced intuitionistic fuzzy c-means (IIFCM) to consider the local spatial information in an intuitively fuzzy manner. To address the limitations of the IFS approach, Yager [18] created a Pythagorean fuzzy set (PFS). PFS developed upon IFS. The PFS add-on expands IFS's use and adaptability of the IFS. With PFS, it can be seen not just how much consensus exists among regions but also how vague that consensus is. Segmenting brain images suggests using an intuitive fuzzy c-means (IFCM) method. Verma suggested enhanced intuitionistic fuzzy c-means (IIFCM) as a novel approach. The authors used IFCM to manage ambiguity. However, the findings indicate that the technique is extremely susceptible to ambiance and makes little use of local spatial data. Improved intuitionistic fuzzy c-means were created to address the insensitivity noise and parameter flexibility selection during tuning. Compared to other existing approaches, the IIFCM approach significantly improves performance. To take this into account, local spatial information is intuitively fuzzy.

Peng et al. [19] investigated the properties of PF aggregation operators, including rigidity, inertia, and predictability. Furthermore, the researchers suggested a PF ranking system based on a scale of excellence and incompetence for addressing MAGDM issues, such as ambiguity and an abundance of attributes. Careful analysis of the PFSMs also led to the recommendation of a novel algorithm for decision-making (DM) based on a 'choice matrix' (CHMX) and a weighted CHMX. Operations including complement, union, intersection, addition, multiplication, necessity, and possibility are delineated in PFS.

Group decision-making, a crucial tool for facilitating medical diagnosis, has been proposed for application to PFSMs. Due to its computational simplicity, PFSMs will be integrated into hospital information systems to help doctors make well-informed decisions based on symptom values. Guleria and Bajaj [20], Ejegwa and Onasanya [21], Hashim et al. [22], and Srivastava [23] proposed various methods based on soft sets. The standardized Rough Intuitive sets were applied to MRI brain images using the Fuzzy C-Means method. Some recent advancements in SSs and FSSs, as well as their applications in decision-making, are discussed by Ali et al. [24], Feng et al. [25], and Kirisci [26].

The Pythagorean fuzzy c-means method was recently proposed for image segmentation [27, 28]. It used min-max parameters to fuzzify and de-fuzzify the image data and used distance measures for clustering. However, the dependency with min-max is not suitable for all types of image data; therefore, a generalized Pythagorean fuzzy c-mean is proposed to extract the tissues of brain AD images. The method uses histogram peaks as initial centroids that help determine the initial degrees of PFS. Using these initial degrees, constrained fuzzy c-means are applied with the Pythagorean objective function, which reduces clustering errors and provides higher data inclusion than intuitionistic fuzzy sets. Kirisci and Simsek [29] proposed advancements in techniques for addressing group decision-making challenges.

The important contributions of this study are as follows:

- The use of PFS was explored in this study for extracting tissues from Alzheimer's disease images.
- An initial centroid is required for each fuzzy-based clustering technique. In this study, centroids are calculated based on the peaks and valleys of the input image histogram.
- PFS aids in identifying the starting cluster regions, reducing the number of segmentation iterations.
- The rapid convergence of PFS is achieved as the starting centroids are calculated based on the image data itself, and the segmentation accuracy is improved with PFS.

The paper is divided into several sections, starting with the background in Section II, the proposed methodology on PFS in Section III, Experimental procedures and outcomes in Section IV, and a summary and future directions in Section V.

2. BACKGROUND

2.1 Intuitionistic fuzzy sets

Membership, non-membership, and hesitancy values are essential in intuitionistic fuzzy sets [8]. Elements are considered members of a cluster or not based on the extent to which they fit within that cluster. A pixel's hesitancy indicates the difficulty of its membership in a certain cluster. Combined with doubt, the fuzzy sets' imprecise knowledge becomes more precise.

$$I=\{(f, \mu_\beta(f), \vartheta_\beta(f)) \mid f\in S\} \quad (1)$$

With $\pi_\alpha(f)=1-(\mu_\beta(f), +\vartheta_\beta(f))$ where the functions $\mu_\beta(f)$, $\vartheta_\beta(f)$ indicates the degree of belonging and non-belonging an ingredient in the realm of finite sets S. $\pi_\beta(f)$ is the determinant of the intuitionistic fuzzy index, which represents an element's degree of uncertainty. The necessary conditions to be satisfied for element, the formula for an IFS-defining $f \in S$ is: $0\leq\mu_\beta(f), \vartheta_\beta(f), \pi(f) \leq 1$. These three functions accurately depict the bias, noise, and cluster to which each element is assigned.

2.2 PFS

One type of fuzzy set is the Pythagorean fuzzy set, a cutting-edge version of the intuitive fuzzy set, and it is used to model

the ambiguity that arises in the actual world when Membership plus non-membership adds up to more than 1. Membership satisfying condition alpha and non-membership satisfying condition beta as $\alpha^2+\beta^2\leq 1$. Figure 1 shows the determinant of PFS.

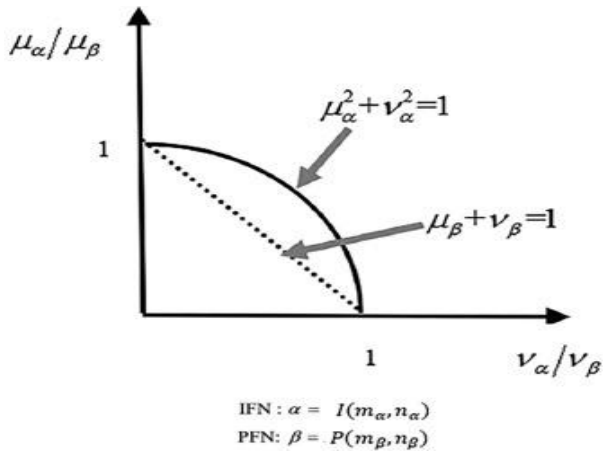

Figure 1. Comparison of IFS and PFS [29]

Definition 1: ADNI dataset [30] considered the universe of conversation as X. The formula for a PFS in X is:

$$I=\{(f, \mu_\alpha(f), \vartheta_\alpha(f)) \mid f\in S\} \quad (2)$$

where, $\mu_\alpha(f)$: X→[0, 1] designation of membership status xεX and $\vartheta_\alpha(f)$: X→[0, 1] symbolizing the extent to which the element is not a member of the set P, depending on the fact that $0 \leq(\mu_\alpha(f))^2+(\vartheta_\alpha(f))^2\leq 1$. The level of uncertainty is given by:

$$\pi_\alpha(x)=\sqrt{(1-(\boldsymbol{\mu_\alpha}(f)^2+\boldsymbol{\vartheta_\alpha}(f)^2)} \quad (3)$$

The main advantages of the PFS over the IFS are described in Table 1. The PFS is more effective in handling vagueness, imprecision, ambiguity, and inconsistency in the data. Hence, the PFS effectively manages noise, bias, and inconsistency in clustering.

Table 1. Comparison of fuzzy, IFS, and PFS

Models	Vagueness	Imprecision	Ambiguity	Inconsistency
Fuzzy	Yes			
IFS	Yes	Yes		
PFS	Yes	Yes	Yes	Yes

2.3 Data sets

There are different data sets available in ADNI [30] based on the stages of Alzheimer's.

Mild dementia: In this stage memory loss of recent events and difficulty with problem-solving are the problems experienced.

Moderate dementia: In this stage, patients experience even greater memory loss and need help from others for their daily activities.

Severe dementia: In this stage, AD affects people who lose the ability to communicate coherently.

For this proposed work, we use the ADNI dataset, which includes three AD images from various categories for experimentation and evaluation. The dataset comprises 200 AD images representing mild, moderate, and severe dementia. The sample images are shown in Figure 2.

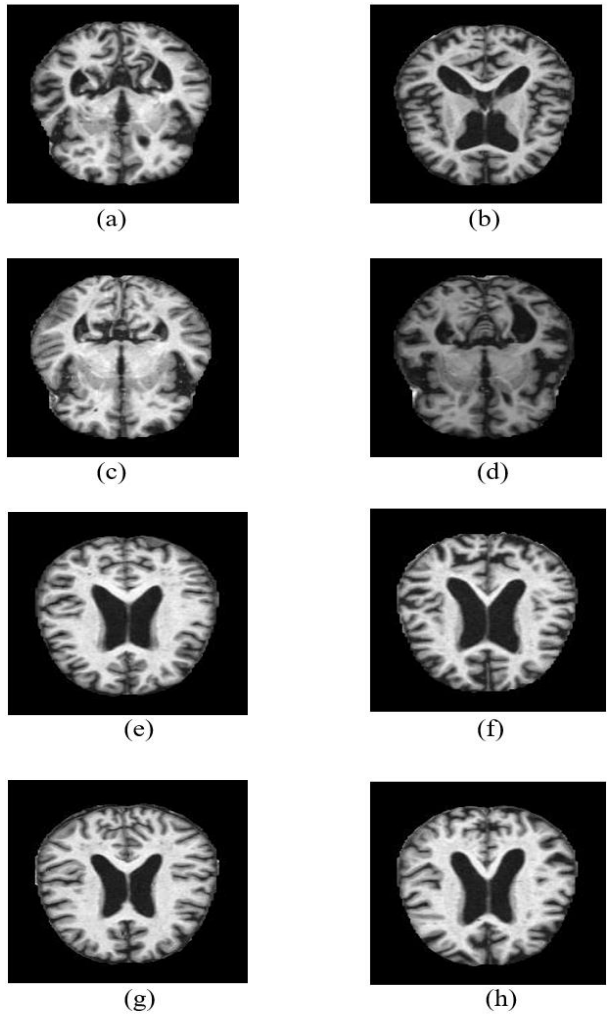

Figure 2. The Alzheimer's dataset images (a, e) Non-dementia (b, f) moderate (c, g) very mild (d, h) mild

3. PROPOSED METHODOLOGY

This chapter focuses mostly on the process of segmenting brain MRI images utilizing PFS. Clustering always depends on the membership function and no single membership function suits all datasets. Hence, to avoid the dependency with the membership we used an approach to calculate initial regions with the image data itself using the thresholds computations [9] and initial centroids using histogram. By identifying the key areas independently of the membership functions used as data for the Pythagorean fuzzy c-means, the proposed method offers a fresh perspective. Further, the approach used the histogram peaks and valleys to determine the initial centroids for the clusters which assists in avoiding the cluster mistakes that occur with random selection. With the proposed method the clustering mistakes are reduced and the dependency on the membership functions is eliminated. Also, the Pythagorean fuzzy c-means has the advantage of addressing ambiguity and uncertainty in the data compared to IFS and offers broader data representation. The detailed process of the proposed method is explained in Figure 3.

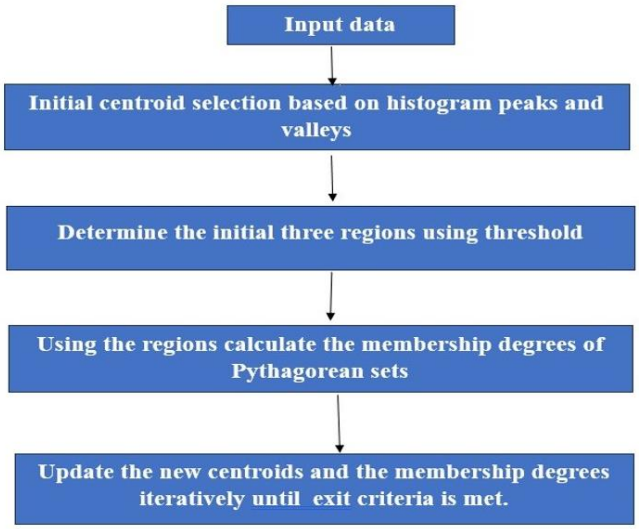

Figure 3. The flow of the proposed method of work

With the histogram peaks calculation, the peaks of brain images are computed and these are used as initial centroids for clustering mentioned in section 3.1. Also, three initial regions are determined by calculating the thresholds obtained from the brain image as presented in section 3.2 continued by the updated constrained partition fuzzy Pythagorean fuzzy c-means for performing the clustering. The primary difference between IFS and PFS lies in the degree of uncertainty measurement given in Eq. (3). The intuitionistic fuzzy c-means clustering is modified to apply the uncertainty equation of PFS.

3.1 Histogram-based initial centroid selection

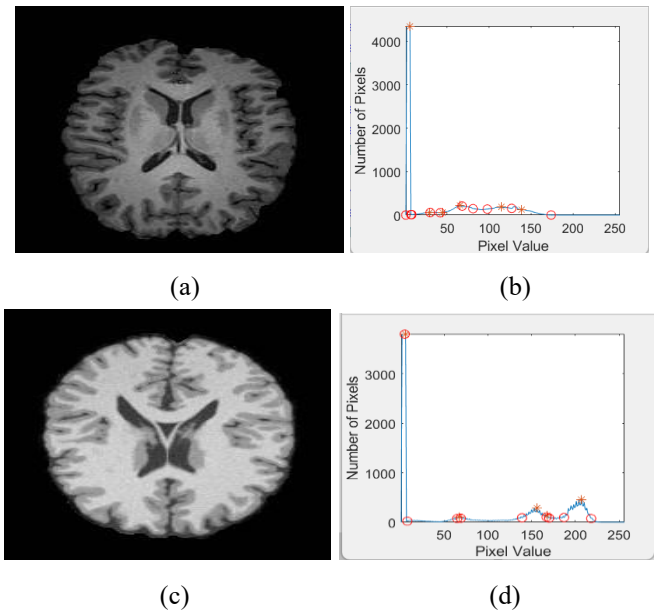

Figure 4. (a, c) ADNI sample Image (b, d) image valleys and peaks

The clustering algorithms are significantly sensitive to the initial cluster. To identify the regions based on distance, the initial centroids are calculated from the histogram peaks. The calculation of histogram peaks is given in previous study [25]. The sample Figure 4 displays the brain images and corresponding prominent peaks and valleys labelled. The author proposed to use the peaks of each histogram as the initial centroids as the peak represents the most repeated value and the bin around it represents the proximity of values near the cluster. Choosing the peaks as initial centroids will give stable regions initially that avoid the problem of local minima (usually occurs when wrong centroids are used).

3.2 Determination of Pythagorean fuzzy regions

Since Fuzzy membership functions are crucial for making clusters, they have a large effect on segmentation efficiency. The initial cluster regions are determined by pixel thresholds calculated with the distances. Let the image of size m×n, is represented as E={P(x)/P(x) indicates pixel value of the i^{th} image element}.

First, the distance between each pixel $P(x)$ to unique intensity values of the image L_k is calculated using Eq. (4) given below:

$$d_i(k) = \frac{\sqrt{\sum_{k \epsilon N\, H_i} (x_i - L_k) \Big/ |N\, H_i|}}{L_{max} - L_{min}} \tag{4}$$

where, $N\,H_i$ is the area surrounding the pixel x_i and $|\,N\,H_i\,|$ is the number of distinct pixels in the image. L_{max} reaches the maximum intensity and L_{min} is the least intensity value. A distance vector can be calculated using this formula $d_i(k)=\{d_i(L_1), d_i(L_2)\ ..., d_i(L_k)\}$ each x_i^{th} pixel. To estimate two thresholds, we employ the maximum and minimum distances, respectively denoted by d_{imax} and d_{imin}.

$$t1 = \frac{1}{M * N} \sum_{i=1}^{M*N} d_{imin} \tag{5}$$

$$t2 = \frac{1}{M * N} \sum_{i=1}^{M*N} d_{imax} \tag{6}$$

The *t1* values show how far apart on average the pixels are from the center of each cluster, whereas the *t2* values show how far apart on average the pixels are from the furthest edges of the clusters. These thresholds serve to estimate three membership functions of the PFS. The belonging region $B(P_x)$, non-belonging $NB(P_x)$, and in-deterministic $I(P_x)$.

If a pixel's distance to a cluster obtained in the histogram, denoted by the symbol $d_i(C_j)$, is smaller than the threshold value t1, then the pixel most likely belongs to the cluster and hence, is located in the determined region $B(C_j)$. Pixels in the $NB(C_j)$ hesitancy region have distances between *t1* and *t2*, indicating that they might either be part of the cluster or not. A pixel is considered to be outside of the cluster and outside of the deterministic region $I(C_j)$ if its distance from the cluster center is larger than the threshold value *t2*. As a result, the pixels can be roughly divided into three regions using these thresholds.

$$x_i = \begin{cases} B(C_j); if\, d_i(C_j) \le t1 \\ N(C_j); if\ t1 \le d_i(C_j) \le t2 \\ I(C_j); otherwise \end{cases} \tag{7}$$

The computation of membership value $\alpha_P(x)$ of the PFS is calculated using the pixels in the $B(C_j)$ using Eq. (8).

$$\alpha_P(x) = \frac{1}{\sum_{j=1}^{n}\left(\frac{\|B_p(x) - C_j\|}{\sum_{c=1}^{n,c!=j}\|B_p(x) - C_c\|}\right)^{2/m-1}} \quad (8)$$

where, C_j represents the center of the j[th] cluster. Here, N $B_P(x)$, and $\pi_P(x)$ are derived from the triangular membership function, and C_c is the arithmetic mean of $B_P(x)$ and C_c, representing the values of the centroid of areas that do not cluster into j[th]. Eqs. (8)-(10) may be used to calculate $\pi_P(x)$ and $\gamma_P(x)$ from $\pi_P(x)$ and $NB_P(x)$, respectively.

$$\beta_P(x) = \frac{1}{\sum_{j=1}^{n}\left(\frac{\|H(e_i) - C_j\|}{\sum_{c=1}^{n,c!=j}\|H(e_i) - C_c\|}\right)^{2/m-1}} \quad (9)$$

$$\pi_p(x) = \sqrt{1 - \left(\alpha_p(x)\right)^2 + \left(\beta_p(x)\right)^2} \quad (10)$$

The following equations are used to revise the PFS partition matrix $\mu_{PFS}P(x)$ and the cluster centroid $C(\mu_P(x))$.

$$\mu_{PFS}P(x) = \alpha^2_P(x) + \beta^2_P(x) + \pi^2_P(x) \quad (11)$$

With the PFS partitioning matrix, the uncertainty of the pixels is modelled and this allows the pixels to more accurately participate in clustering.

$$C\left(\mu(p(x))\right) = \frac{\sum_{p(x)\epsilon E}\left(\mu(p(x))\right)^m (p(x))}{\sum_{p(x)\epsilon E}\left(\mu(p(x))\right)^m} \quad (12)$$

Use Eq. (12) to locate the missing centroids for $\pi(p(x))$ and $\gamma(p(x))$. The user-specified fuzzification constant is denoted here by m. A sharp and binary membership function is obtained if m is near 1; otherwise, it becomes fuzzy and blurry as m increases [22]. With, large datasets that can be successfully segmented 1.5<m<3 plus 2 is typically thought of [23, 24]. Like many other clustering techniques, Pythagorean fuzzy c-means relies on iterative refinement. Repeatedly applying Eqs. (4)-(6) to identify the three regions and Eq. (8) to obtain the new centroids, the process concludes once the clusters reach stability. Stability in a cluster is determined by a Hamming distance between the first set of clusters and a similarity coefficient $\mu_{PFS}P(x)^l$ and $\mu_{PFS}P(x)^{l+1}$. The formula for the hammering distance is:

$$SC = \sum_{i=1}^{M*N} |\mu_{PFS}P(x)^l - \mu_{PFS}P(x)^{l+1}| \quad (13)$$

3.3 PFCM algorithm for tissue segmentation

In this section, the steps of the PFCM clustering are proposed. The following Algorithm 1 describes the steps for the segmentation of brain tissues.

Algorithm1

I/P: Input image P and ϵ Cutoffs at 0.01.

O/P: The Values of x, y, and z for the region of the brain image are used to build the n clusters that will represent those regions.

1. Compute the initial cluster of centroids
   Cj = FINDPEAKS(X, n)
2. Put 0 in the $\mu_{IFS}(x_i)l$ as a starting point
   for all x_i of NH varying intensities. do
   using Eq. (4), determine the distance in $d_i(k)$
   end for
   end for
3. Find the two thresholds t1 and t2 using Eq. (5).
4. Determine the regions using Eq. (7).
5. While 1 do
   5.1 Using Eqs. (8)-(10), we can derive three intuitive estimates for the membership function.
   5.2 Alter the partition matrix μ_{PFS}(P(x)) and the centroid of the cluster, C_j, via Eq. (11) and Eq. (12).
   5.3 For a rough estimation of the similarity coefficient (sc),
   use the formula: Eq. (13).
   5.4 if sc ≤ ϵ then then
   break
   else
   $\mu_{PFS}(P(x))^l = \mu_{PFS}(p(x))^{l+1}$
   end if
   5.5 end while
6. With stable α(P(x)), β(P(x)) and π(P(x)) obtain n clusters.

---

4. EXPERIMENTAL PROCEDURES AND OUTCOMES

4.1 Context for experiment

The ADNI dataset was used to evaluate the proposed PFCM method. Brain images, including diagnostic, clinical, technical, and database attribute images, were included in the data collection. The PFCM algorithm presented in this study was developed in MATLAB, using an i5 CPU. The proposed approach for identifying the three zones assigns a value of 3 to the total number of clusters, n. The generalization process served as the initializer for the centroid values. The exit criterion is a constant of 0.01 standard deviations from the next cluster. Since the ADNI dataset contains brain images in different formats—MPRAGE, FLAIR, and DTI, which are available in various sizes—the images were converted to a MATLAB-readable format using the MIPAV tool. The skull portion of the brain was removed using MIPAV's brain extraction tool. Additionally, as part of the pre-processing phase, the images were resized to a standard 512×640 pixels.

Post-processing in the proposed algorithm involves converting the final segmented regions into black and white to compare them with the ground truth. For visualization purposes, colors are applied to the grayscale images to analyze the CSF fluid region, which is relevant in Alzheimer's disease analysis.

Figure 5 shows the results of the PFCM algorithm applied to segment several brain images. Column 1 presents the original ADNI dataset images, Column 2 shows the extracted CSF regions, Column 3 shows gray matter extraction images, and Column 4 shows white matter extraction for the brain images in the ADNI dataset. Because the image sizes for the ADNI datasets vary significantly, they are resized to 512×640 pixels as part of the pre-processing step. The post-processing step involves converting the final segmented regions to black and white to facilitate comparison with the ground truth.

The segmentation results of the proposed algorithm are

shown in Figure 6. Row 1 illustrates the ground truth for gray matter, white matter, and CSF. Row 2 shows GM, WM, and CSF extraction using PFCM, while Row 3 shows the same extraction method using GRIFCM. According to a subjective evaluation, the proposed method effectively extracts brain tissue. The segmentation results of the proposed algorithm are displayed in Figure 7. Based on subjective evaluation, the proposed method proves effective for brain tissue extraction.

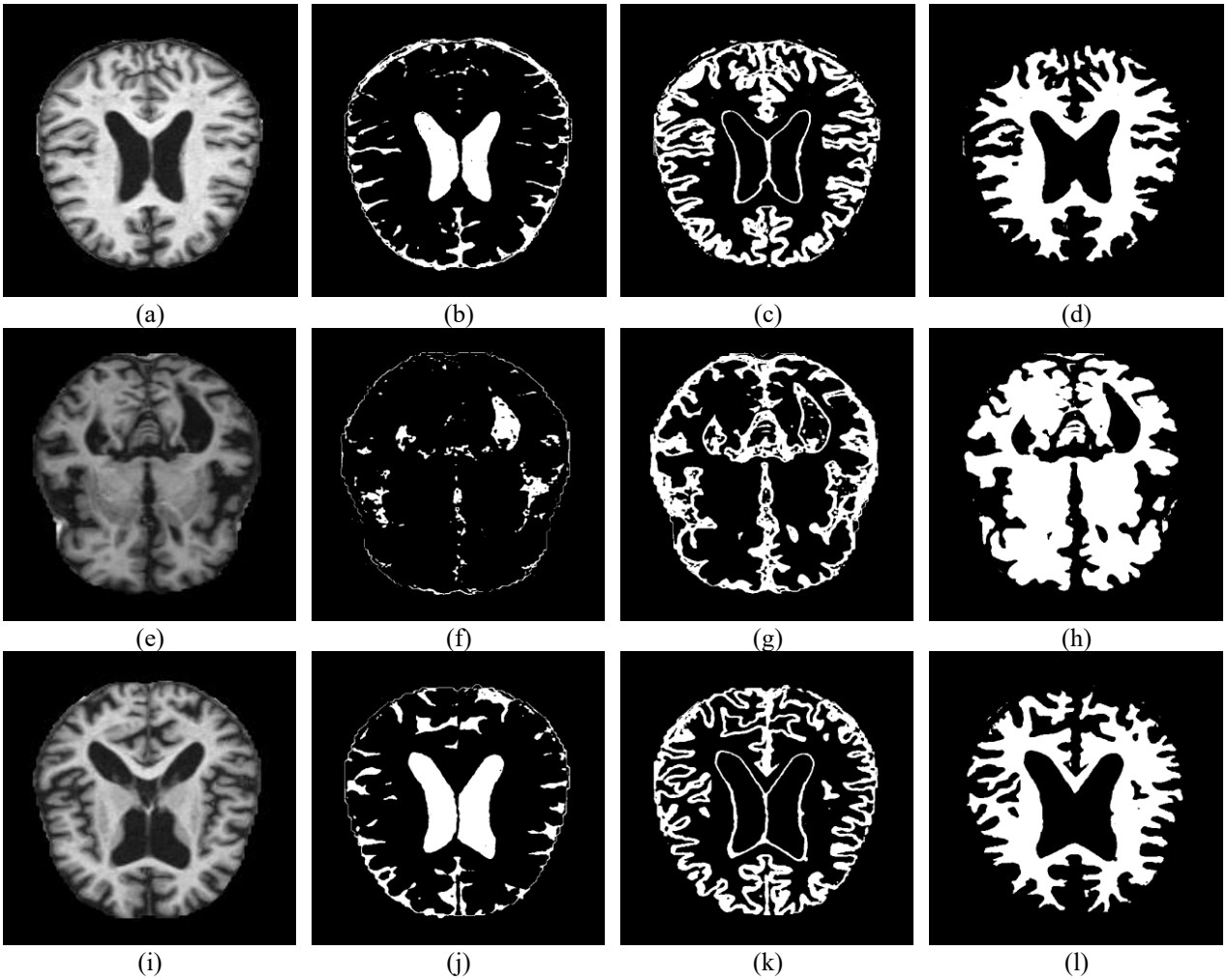

Figure 5. (a) very mild (e) mild (i) moderate images from ADNI data set, (b)(f)(j) CSF extracted, (c)(g)(k) gray matter extracted (d)(h)(l) white matter extracted

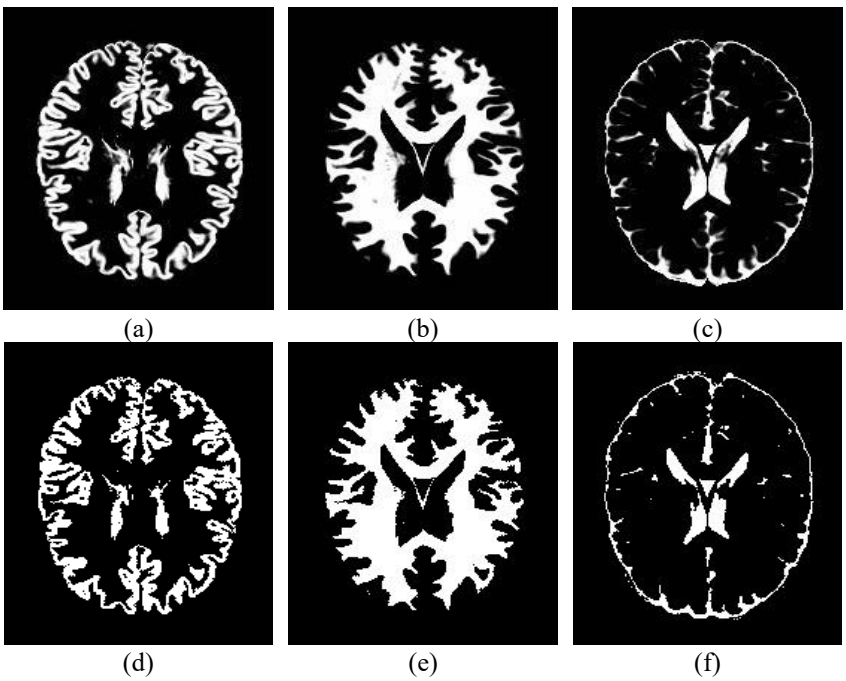

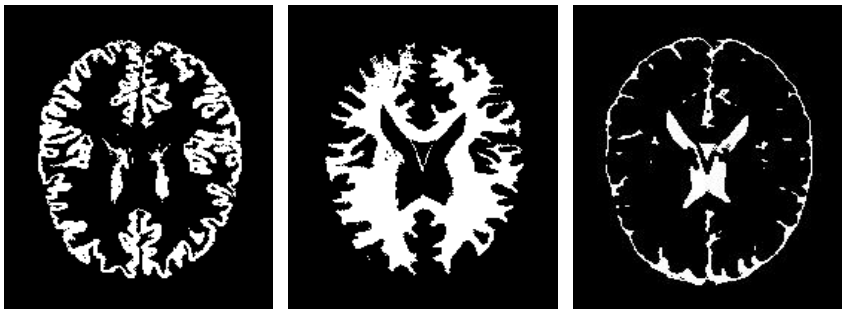

(g) (h) (i)

Figure 6. Segmentation results of proposed algorithm (row 1) ground truths of GM, WM, and CSF, (row 2) GM, WM, and CSF extracted using PFCM (row 3) GM, WM, and CSF extracted using GRIFCM [14]

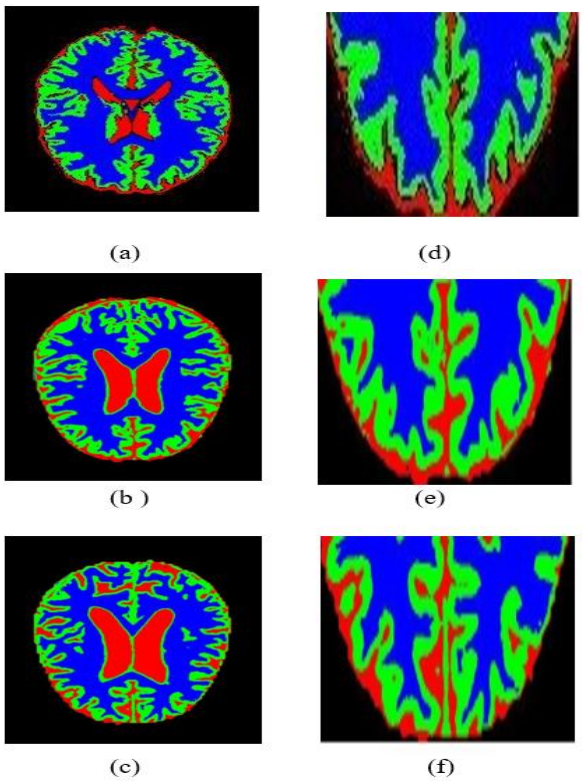

Figure 7. Segmentation results of proposed algorithm PFCM for normal, moderate, and mild Alzheimer's images

4.2 Statistical methods

Measurable metrics such as segmentation accuracy (SA), Jaccard coefficient (JC), and Dice coefficient (DC) are used to verify the performance of the proposed model. The performance of most classification or clustering algorithms is assessed using SA, JC, DC, precision, specificity, and sensitivity. Metrics closer to 1 indicate high performance. If the value is above 0.7 (or 70%), the model is considered to be performing well. As the metrics approach 1 or 100%, the model demonstrates improved performance.

$$\text{Jaccard\_coefficient} = \frac{A \cap B}{A \cup B} \tag{14}$$

$$\text{Dice\_coefficient} = \frac{2\,|\,A \cap B\,|}{|\,A\,| + |\,B\,|} \tag{15}$$

in which, A is an original image on the ground. The resulting segmented image is represented by B.

$$\text{Segmentation Accuracy(SA)} = \frac{TP + FN}{TP + TN + FP + FN} \tag{16}$$

$$\text{Sensitivity} = TP/(TP + FN) \tag{17}$$

$$\text{Specificity} = TN/(TN + FP) \tag{18}$$

$$\text{Precision} = TP/(TP + FP) \tag{19}$$

where,

(1). True positive (TP): Quantity of the B's actual pixels as seen in A expressed as a ratio.

(2). True negative (TN): Negatively segmented true pixels in B as a ratio to the total number of pixels in A.

(3). False positive (FP): Sum of incorrect positive pixels segmented in B as negative and vice versa.

(4). False negative (FN): The percentage of B images where negative values were observed in A.

The performance measures of segmentation accuracy, JC, DC sensitivity, specificity, and precision are depicted in Table 2. The extracted tissues are compared with the ground truths of the images to compute the performance measures. The ADNI data sets images of mild, moderate, and severe dementia images from which these performance measures are derived. The outcomes validated the effectiveness of the proposed algorithms in extracting the brain tissue region. With the proposed method, the typical JC score is 0.95, and the SA is 0.98. A Jaccard coefficient (JC) value of 0.8 or higher indicates aesthetic correctness and therefore suggests high-quality segmentation. In a sample of 100 images from ADNI, assuming universal agreement, the JC value is 0.86. Using this sample, we find that observers consistently agree on a JC value of 0.86.

Table 2. Comparative performance metrics

Images	SA	JC	DC	Precision	Sensitivity	Specificity
very mild	0.9864	0.9545	0.9771	0.9842	0.9696	0.9956
Mild	0.9741	0.8633	0.9277	0.8813	0.9768	0.9763
Moderate	0.9814	0.7945	0.8894	0.8278	0.9508	0.9859

Table 3. Measures of effectiveness compared across a range of segmentation algorithms

Algorithm	SA	JC	DC	Sensitivity	Specificity
[26]	0.909	0.7895	0.891	0.736	0.920
[27]	0.910	0.755	0.749	0.815	0.875
[28]	0.912	0.752	0.857	0.830	0.878
[29]	0.884	0.665	0.884	0.869	0.884
[14]	0.972	0.912	0.882	0.920	0.882
PFCM	0.985	0.973	0.891	0.9508	0.891

Table 4. Comparison of algorithm execution times

KM	FCM	RFCM	GRIFCM	PFCM
39.5±2.3	36.8±2.5	33.4±2.1	21.5±3.2	15.56±2.5

Table 3 compares the proposed PFCM approach with advanced methodologies from the literature. As shown in the table below, the suggested approach achieves slightly higher JC values compared to the most advanced techniques for brain segmentation. Values of sensitivity are also improved by the proposed method. Deep learning algorithms have demonstrated remarkable precision and accuracy in this area of research on brain tissue segmentation. However, the performance measures of the proposed method are in line with those acquired by deep learning proving the efficacy of the algorithm concerning performance and time as well.

The widely used FCM categorization of pixels using histogram has shown an accuracy of 88% only as the FCM suffers from noise. Values for SA, JC, precision, and sensitivity are greatly enhanced by the proposed methods, however, values for specificity and DC are reduced. The approach is also compared with the IFCM proposed by Namburu et al. [14], which utilized intuitionistic fuzzy c-means for clustering. Compared to IFCM, the proposed method performs better due to its higher degree of certainty than PFS. Table 4 describes the execution time comparison for different algorithms. The proposed algorithm takes less time than the existing fuzzy-based algorithms as the clustering mistakes are reduced with the certainty membership as the ambiguity and vagueness of the pixels are reduced.

PFS has the advantage of addressing ambiguity, vagueness, and uncertainty in the data, with a higher degree of membership, making it more suitable for extracting brain tissues. The extracted brain tissue further aids in classifying the stages of Alzheimer's.

Alzheimer's is identified by an increase in CSF fluid and shrinkage of white matter. The time series data need to be collected for each patient and the changes in the tissues are verified to state the patient is in which state of AD. The proposed work is limited to segmenting the tissues which further need to be enhanced to classify the AD by using hybrid techniques that can combine the time-series image data and the proposed segmentation algorithm. As the classification of AD is complex with a single image of the brain, hence extracting the tissues and measuring the tissues with a classification model enhances Alzheimer which will be further considered in our later studies.

5. CONCLUSION

Computer-aided detection of Alzheimer's with the use of brain images has tremendously assisted clinicians. Due to numerous factors like artifacts in brain MRI, varied pixel intensity, and images with poor contrast Alzheimer's detection increased complexity. Here, we introduce a novel PFCM algorithm for Segmenting Brain Images. The histogram peaks of the image are used as initial regions and centroids. This avoids the local minima and the initial regions are determined without depending on the membership function making the algorithm generalized. Cluster stability is improved, and runtime is shortened, thanks to the regions' contributions. The extracted regions serve as inputs in the membership function calculations of the Pythagorean fuzzy soft sets clustering handling uncertainty in the brain images. Further, the extracted tissues can be used as input to deep learning models that can classify the Alzheimer's stages more accurately.

ACKNOWLEDGMENTS

All authors have read and agreed to the published version of the manuscript. The authors would like to thank Mohamed Sirajuddin, coordinator, High Performance Computing Lab at VIT-AP University, Amaravathi, Andhra Pradesh, India for his support and Providing resources for the Experimental analysis.

REFERENCES

[1] Weller, J., Budson, A. (2018). Current understanding of Alzheimer's disease diagnosis and treatment. F1000Research, 7: 1161. https://doi.org/10.12688/f1000research.14506.1

[2] Rasmussen, J., Langerman, H. (2019). Alzheimer's disease we need early diagnosis. Degenerative Neurological and Neuromuscular Disease, 2019(9): 123-130. https://doi.org/10.2147/dnnd.s228939

[3] Ahmad, S., Aijaz, M., Ahmad, M., Hafeez, A., Asif, M., Kumar, A., Al-Taie, A., Ansari, M.A. (2023). Early detection of Alzheimer's disease by using the latest techniques. Authorea Preprints.

[4] Morra, J.H., Tu, Z., Apostolova, L.G., Green, A.E., Toga, A.W., Thompson, P.M. (2009). Comparison of AdaBoost and support vector machines for detecting Alzheimer's disease through automated hippocampal segmentation. IEEE Transactions on Medical Imaging, 29(1): 30-43. https://doi.org/10.1109/TMI.2009.2021941

[5] Islam, F., Rahman, M.H., Hossain, M.S., Ahmed, S. (2023). A novel method for diagnosing Alzheimer's disease from MRI scans using the ResNet50 feature extractor and the SVM classifier. International Journal of Advanced Computer Science and Applications, 14(6). https://doi.org/10.14569/IJACSA.2023.01406131

[6] Dzitac, I., Filip, F.G., Manolescu, M.J. (2017). Fuzzy logic is not fuzzy: World-renowned computer scientist Lotfi A. Zadeh. International Journal of Computers Communications & Control, 12(6): 748-789. http://doi.org/10.15837/ijccc.2017.6.3111

[7] Bezdek, J.C., Ehrlich, R., Full, W. (1984). FCM: The fuzzy c-means clustering algorithm. Computers & Geosciences, 10(2-3): 191-203. https://doi.org/10.1016/0098-3004(84)90020-7

[8] Latif, G., Alghazo, J., Sibai, F.N., Iskandar, D.A., Khan,

A.H. (2021). Recent advancements in fuzzy C-means-based techniques for brain MRI segmentation. Current Medical Imaging, 17(8): 917-930. https://doi.org/10.2174/1573405616666210104111218

[9] Ji, Z., Sun, Q., Xia, Y., Chen, Q., Xia, D., Feng, D. (2012). Generalized rough fuzzy c-means algorithm for brain MR image segmentation. Computer Methods and Programs in Biomedicine, 108(2): 644-655. https://doi.org/10.1016/j.cmpb.2011.10.010

[10] Anupama, N., Kumar, S., Reddy, E. (2013). Rough set-based MRI medical image segmentation using optimized initial centroids. International Journal of Emerging Technologies in Computational and Applied Sciences, 6(1): 90-98.

[11] Namburu, A., Srinivas Kumar, S., Srinivasa Reddy, E. (2022). Review of set-theoretic approaches to magnetic resonance brain image segmentation. IETE Journal of Research, 68(1): 350-367. https://doi.org/10.1080/03772063.2019.1604176

[12] Maji, P.K., Roy, A.R., Biswas, R. (2002). An application of soft sets in a decision-making problem. Computers & Mathematics with Applications, 44(8-9): 1077-1083. https://doi.org/10.1016/S0898-1221(02)00216-X

[13] Namburu, A., kumar Samay, S., Edara, S.R. (2017). Soft fuzzy rough set-based MR brain image segmentation. Applied Soft Computing, 54: 456-466. https://doi.org/10.1016/j.asoc.2016.08.020

[14] Namburu, A., Samayamantula, S.K., Edara, S.R. (2017). Generalized rough intuitionistic fuzzy c-means for magnetic resonance brain image segmentation. IET Image Processing, 11(9): 777-785. https://doi.org/10.1049/iet-ipr.2016.0891

[15] Atanassov, K.T. (1986). Intuitionistic fuzzy sets. Fuzzy Sets and Systems, 20(1): 87-96. https://doi.org/10.1016/S0165-0114(86)80034-3

[16] Dubey, Y.K., Mushrif, M.M., Mitra, K. (2016). Segmentation of brain MR images using rough set-based intuitionistic fuzzy clustering. Biocybernetics and Biomedical Engineering, 36(2): 413-426. https://doi.org/10.1016/j.bbe.2016.01.001

[17] Verma, H., Agrawal, R.K., Sharan, A. (2016). An improved intuitionistic fuzzy c-means clustering algorithm incorporating local information for brain image segmentation. Applied Soft Computing, 46: 543-557. https://doi.org/10.1016/j.asoc.2015.12.022

[18] Yager, R.R. (2013). Pythagorean membership grades in multicriteria decision making. IEEE Transactions on Fuzzy Systems, 22(4): 958-965. https://doi.org/10.1109/TFUZZ.2013.2278989

[19] Peng, X., Yang, Y., Song, J., Jiang, Y. (2015). Pythagorean fuzzy soft set and its application. Computer Engineering, 41(7): 224-229. http://doi.org/10.3969/j.issn.1000-3428.2015.07.043

[20] Guleria, A., Bajaj, R.K. (2019). On Pythagorean fuzzy soft matrices, operations and their applications in decision making and medical diagnosis. Soft Computing, 23: 7889-7900. https://doi.org/10.1007/s00500-018-3419-z

[21] Ejegwa, P.A., Onasanya, B.O. (2019). Improved intuitionistic fuzzy composite relation and its application to the medical diagnostic process. Notes on Intuitionistic Fuzzy Sets, 25(1): 43-58. https://doi.org/10.7546/nifs.2019.25.1.43-58

[22] Hashim, R.M., Gulistan, M., Rehman, I., Hassan, N., Nasruddin, A.M. (2020). Neutrosophic bipolar fuzzy set and its application in medicines preparations. Neutrosophic Sets and Systems, 31: 86-100.

[23] Srivastava, A. (2019). Medical diagnosis using intuitionistic fuzzy sets. Emerging Trends in Mathematical Sciences and its Applications, AIP Publishing LLC, 2061(1): 020029. https://doi.org/10.1063/1.5086651

[24] Ali, M.I., Feng, F., Liu, X., Min, W.K., Shabir, M. (2009). On some new operations in soft set theory. Computers & Mathematics with Applications, 57(9): 1547-1553. https://doi.org/10.1016/j.camwa.2008.11.009

[25] Feng, F., Fujita, H., Ali, M.I., Yager, R.R., Liu, X. (2018). Another view on generalized intuitionistic fuzzy soft sets and related multiattribute decision-making methods. IEEE Transactions on Fuzzy Systems, 27(3): 474-488. https://doi.org/10.1109/TFUZZ.2018.2860967

[26] Kirişci, M. (2020). Medical decision-making to the fuzzy soft sets. Journal of Interdisciplinary Mathematics, 23(4): 767-776. https://doi.org/10.1080/09720502.2020.1715577

[27] Ma, R., Zeng, W., Song, G., Yin, Q., Xu, Z. (2021). Pythagorean fuzzy C-means algorithm for image segmentation. International Journal of Intelligent Systems, 36(3): 1223-1243. https://doi.org/10.1002/int.22339

[28] Gayen, S., Biswas, A. (2021). Pythagorean fuzzy c-means clustering algorithm. In International Conference on Computational Intelligence in Communications and Business Analytics. Cham: Springer International Publishing. Springer, Cham, pp. 118-130. https://doi.org/10.1007/978-3-030-75529-4_10

[29] Kirişci, M., Şimşek, N. (2022). Decision-making method related to Pythagorean Fuzzy Soft Sets with infectious diseases application. Journal of King Saud University-Computer and Information Sciences, 34(8): 5968-5978. https://doi.org/10.1016/j.jksuci.2021.08.010

[30] ADNI dataset. https://adni.loni.usc.edu/data-samples/adni-data/.